Nuclear magnetic resonance spectroscopy with the stringent substrate rhodanese bound to the single-ring variant SR1 of the E. coli chaperonin GroEL

ARTICLE *in* PROTEIN SCIENCE · AUGUST 2011

Impact Factor: 2.85 · DOI: 10.1002/pro.665 · Source: PubMed

4 AUTHORS, INCLUDING:

Reto Horst
Pfizer Inc.
30 PUBLICATIONS **964** CITATIONS
SEE PROFILE

Arthur L Horwich
Yale University
173 PUBLICATIONS **19,505** CITATIONS
SEE PROFILE

Kurt Wüthrich
The Scripps Research Institute
742 PUBLICATIONS **75,994** CITATIONS
SEE PROFILE

Nuclear Magnetic Resonance spectroscopy with the stringent substrate rhodanese bound to the single-ring variant SR1 of the *E. coli* chaperonin GroEL

Eda Koculi,[1] Reto Horst,[1] Arthur L. Horwich,[1,2,3] and Kurt Wüthrich[1,4]*

[1]Department of Molecular Biology, The Scripps Research Institute, La Jolla, California 92037
[2]Howard Hughes Medical Institute, Yale University School of Medicine, New Haven, Connecticut 06510
[3]Department of Genetics, Yale University School of Medicine, New Haven, Connecticut 06510
[4]The Skaggs Institute of Chemical Biology, The Scripps Research Institute, La Jolla, California 92037

Received 14 April 2011; Accepted 12 May 2011
DOI: 10.1002/pro.665
Published online 1 June 2011 proteinscience.org

Abstract: Nuclear magnetic resonance (NMR) observation of the uniformly ^{2}H,^{15}N-labeled stringent 33-kDa substrate protein rhodanese in a productive complex with the uniformly ^{14}N-labeled 400 kDa single-ring version of the *E. coli* chaperonin GroEL, SR1, was achieved with the use of transverse relaxation-optimized spectroscopy, cross-correlated relaxation-induced polarization transfer, and cross-correlated relaxation-enhanced polarization transfer. To characterize the NMR-observable parts of the bound rhodanese, coherence buildup rates by different magnetization transfer mechanisms were measured, and effects of covalent crosslinking of the rhodanese to the apical binding surface of SR1 were investigated. The results indicate that the NMR-observable parts of the SR1-bound rhodanese are involved in intracomplex rate processes, which are not related to binding and release of the substrate protein from the SR1 binding surface. Rather, they correspond to mobility of the stably bound substrate, which thus appears to include flexibly disordered polypeptide segments devoid of long-lived secondary structures or tertiary folds, as was previously observed also with the smaller substrate human dihydrofolate reductase.

Keywords: protein folding; TROSY; CRINEPT; coherence transfer; substrate protein–chaperonin crosslinking

Introduction

Information on the conformational states adopted by substrate proteins while captured inside an open ring of the chaperonin GroEL is of keen interest, because this structural state reflects both on the ability of GroEL to prevent or rescue non-native polypeptides from misfolding and irreversible aggregation by binding them and on the ability of the chaperonin to subsequently direct folding to the physiologically active state on binding of ATP and GroES to the same ring that contains the substrate.[1–3] As concerns binding, the seven hydrophobic cavity-facing apical surfaces of an open GroEL

Abbreviations: CRIPT, cross-correlated relaxation-induced polarization transfer; hDHFR, human dihydrofolate reductase; HMQC, heteronuclear multiple-quantum coherence; HSQC, heteronuclear single-quantum coherence; INEPT, insensitive nuclei enhanced by polarization transfer; TROSY, transverse relaxation-optimized spectroscopy; SR1, single-ring variant of *E. coli* GroEL.

Eda Koculi and Reto Horst contributed equally to this work

**Correspondence to:* Kurt Wüthrich, Department of Molecular Biology, The Scripps Research Institute, La Jolla, CA 92037. E-mail: wuthrich@scripps.edu

ring enable multivalent binding of a non-native substrate protein through exposed hydrophobic surfaces of the substrate, which will become buried in the native state.[4–10] Such binding to GroEL prevents interactions between these hydrophobic surfaces that may otherwise lead to self-aggregation.[11] There seems to be thermodynamic partitioning, in which binding by GroEL of conformers with large amounts of exposed hydrophobic surface shifts an ensemble of non-native states toward those exposing the greatest amount of hydrophobic surface.[12,13] It has also been suggested that passive "stretching" exerted on the chain topology, as evidenced in fluorescence studies,[14] may further optimize the extent of hydrophobic surface interactions.

Protein bound in an open ring of GroEL is accessible to reaching the native fold on subsequent binding of ATP and GroES to the same ring. ATP/GroES binding produces large rigid-body movements of the GroEL apical domains, which thus displace their hydrophobic binding surface away from the bound polypeptide, releasing substrate polypeptide into the so called cis folding chamber, where folding to the native fold can occur in an isolated hydrophilic environment, without the possibility of self-aggregation.[15–20]

Here, we continue investigations on the potentialities of solution nuclear magnetic resonance (NMR) techniques for characterization of the conformational state of stably GroEL-bound substrate proteins, using a 433-kDa binary complex containing the uniformly ^{2}H,^{15}N-labeled stringent 33 kDa substrate bovine rhodanese[15,21–23] and the uniformly ^{14}N-labeled 400 kDa single-ring version of GroEL known as SR1.[24] These experiments extend an earlier NMR study of SR1 complexed with the 21-kDa substrate human dihydrofolate reductase (hDHFR), which showed that the NMR-observable parts of the bound hDHFR were devoid of native-like globular structure.[25] In the present experiments, rhodanese represents a protein with more typical size of GroEL/GroES-requiring substrates. Rhodanese is also a stringent substrate protein, that is, in contrast to hDHFR it is unable, in the absence of the chaperonin, to produce the native fold on dilution from denaturant at neutral pH and 22°C, which leads instead to nonspecific aggregation.

Results and Discussion

Two-dimensional cross-correlated relaxation-enhanced polarization transfer–heteronuclear multiple-quantum coherence–[^{1}H]-transverse relaxation-optimized NMR spectrum of a noncovalent rhodanese–SR1 binary complex

To form a rhodanese–SR1 binary complex, [u-^{15}N, u>98% ^{2}H]-rhodanese was diluted from 8*M* urea into a buffer containing [u-^{14}N]-SR1, as described in Materials and Methods section. ^{15}N-depleted SR1 was used to assure that signals in the [^{15}N,^{1}H]-correlation NMR spectra would be produced solely by ^{15}N-labeled rhodanese, without possible admixture of spurious signals from the natural-abundance ^{15}N that would otherwise be present in SR1. Exploratory experiments had shown that highest sensitivity for observation of SR1-bound rhodanese was obtained with the two-dimensional (2D) [^{15}N,^{1}H]-cross-correlated relaxation-enhanced polarization transfer (CRINEPT)–heteronuclear multiple-quantum coherence (HMQC)–[^{1}H]-transverse relaxation-optimized spectroscopy (TROSY) experiment [Fig. 1(A)].[26–28] In this experiment, the combined use of TROSY during [^{1}H]-evolution and CRINEPT during polarization transfer steps enables the recording of 2D [^{15}N,^{1}H]-correlation maps for polypeptide segments with variable mobility in molecular assemblies with sizes up to 1 MDa.[26] In the 2D [^{15}N,^{1}H]-CRINEPT–HMQC–[^{1}H]-TROSY spectrum of [u-^{15}N, u∼98% ^{2}H]-rhodanese in complex with SR1 [Fig. 1(A)], most of the signals are within the ^{1}H chemical shift range of 7.5–8.5 ppm, the exception being signals from amino acid side chains with ^{1}H shifts of 6.5–7.5 ppm (see next section). These observations indicate that the NMR-observable parts of the protein do not adopt either long-lived secondary structures or tertiary folds, which corroborates earlier work with different substrate proteins.[25,29] Because of the small chemical shift dispersion, the NMR signals are overlapped in clusters, so that it is difficult to estimate the number of residues observed in the spectrum of Figure 1(A). In the following sections, we used additional NMR experiments and biochemical studies of the rhodanese–SR1 complex to support a more detailed interpretation of the data in Figure 1(A) and to assess their biological relevancy.

Comparison of two-dimensional ^{15}N–^{1}H correlation experiments with different transverse relaxation-optimization schemes

In contrast to the 2D [^{15}N,^{1}H]-CRINEPT–HMQC–[^{1}H]-TROSY experiment, fast transverse relaxation in 2D [^{15}N,^{1}H]-heteronuclear single-quantum coherence (HSQC)[30] and to a lesser extent in 2D [^{15}N,^{1}H]-TROSY[31] measurements with particles of several hundred kDa in size ensures that the cross-peaks visible in the resulting spectra can be attributed to polypeptide segments with significant intramolecular mobility, in addition to the overall tumbling of the large molecular assembly. For the backbone amide signals, with ^{1}H chemical shifts from 7.5 to 8.5 ppm in the 2D [^{15}N,^{1}H]-HSQC spectrum of [u-^{15}N, u∼98% ^{2}H]-rhodanese in complex with SR1 [Fig. 1(C)], we can resolve about 25 cross-peaks, and there are approximately 35 cross-peaks in the 2D [^{15}N,^{1}H]-TROSY spectrum [Fig. 1(B)]. Overall, about

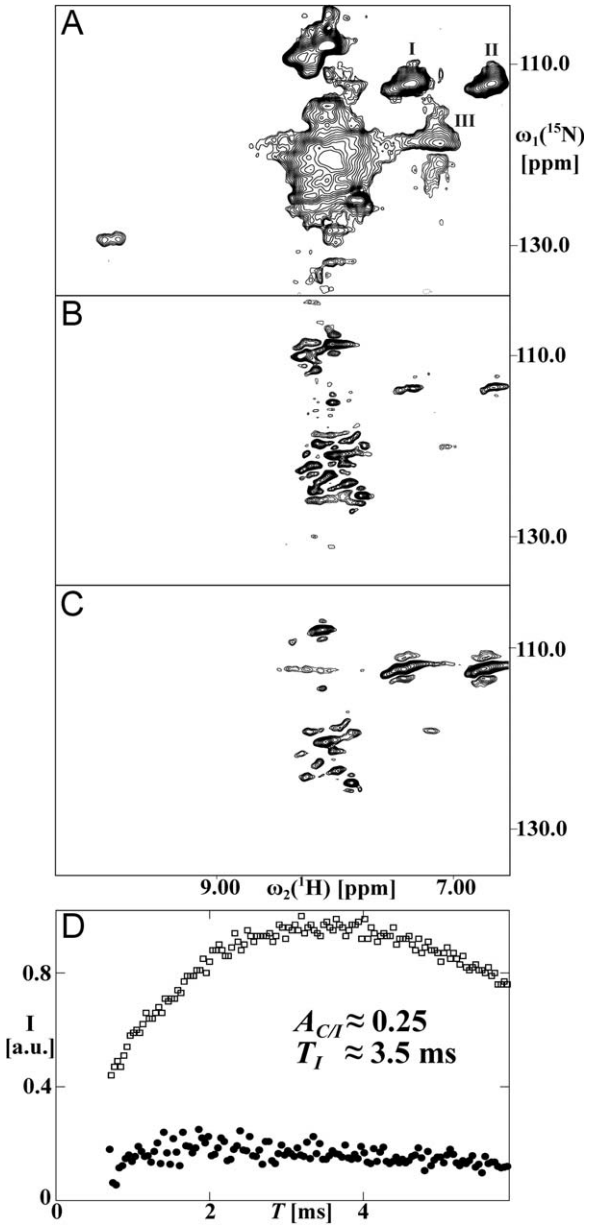

Figure 1. NMR characterization of [u-^{15}N, u-98% ^{2}H]-rhodanese bound to [u-100% ^{14}N]-SR1 with the following experiments: (A) 2D [^{15}N,^{1}H]-CRINEPT–HMQC–[^{1}H]-TROSY. The peak clusters for the side-chain ^{15}N–$^{1}H_2$ groups of Gln and Asn are indicated by I and II, and the peak from an Arg $N^{\varepsilon}H^{\varepsilon}$ side-chain amide moiety is indicated by III. (B) 2D [^{15}N,^{1}H]-TROSY. (C) 2D [^{15}N,^{1}H]-HSQC. The acquisition and processing parameters are given in Materials and Methods section. (D) Experimental transfer efficiencies for CRIPT (filled circles) and INEPT (open squares) at variable lengths of the transfer period *T*. The data were derived from the intensity of the signals in the ^{1}H chemical shift range between 8.0 and 8.3 ppm of rhodanese in complex with SR1. Relative signal intensities, *I*, are plotted versus *T*. The parameters used to assess the internal dynamics, that is, the ratio between the optimal CRIPT and INEPT transfer efficiencies, $A_{C/I}$, and the optimal INEPT transfer delay, T_I, are indicated. The NMR experiments used to collect this data are described in Materials and Methods section.

15% of the peaks expected from the amino acid sequence of rhodanese are thus observed with TROSY [Fig. 1(B)], with about 10% having sufficiently high flexibility within the SR1 complex to be observable in the HSQC spectrum [Fig. 1(C)] and an additional 5% with restricted mobility. Two peak clusters with ^{1}H chemical shifts of 7.5 and 6.5 ppm [indicated by I and II in Fig. 1(A)] are from the Asn and Gln side-chain NH_2 moieties. They are almost completely suppressed by the ST2-PT segment of the 2D [^{15}N,^{1}H]-TROSY experiment.[32] Comparison with the 2D [^{15}N,^{1}H]-TROSY and 2D [^{15}N,^{1}H]-HSQC spectra suggests that the 2D [^{15}N,^{1}H]-CRINEPT–HMQC–[^{1}H]-TROSY spectrum contains signals also from largely immobilized segments of the substrate protein. The large line widths and the severe overlap of the resonances in the spectrum of the binary complex make it difficult to estimate the number of resonances observed in Figure 1(A). Assuming that all of the side-chain NH_2 groups of Asn and Gln contribute to the peak clusters indicated by I and II in Figure 1(A), we estimate that the intensities of the other peaks in Figure 1(A) represent 80 backbone ^{15}N–^{1}H moieties of the bound rhodanese, which corresponds to about 30% of the expected cross-peaks.

An interesting feature in Figure 1(A) is the appearance of an intense Arg side-chain cross-peak, indicated by III in Figure 1(A), which had very weak intensity in the 2D [^{15}N,^{1}H]-TROSY and the 2D [^{15}N,^{1}H]-HSQC spectra [Fig. 1(B) and (C)]. There is thus at least one Arg side chain with restricted mobility, indicating salt bridge formation in the bound state of the substrate.

Coherence buildup by different magnetization transfer schemes

To further characterize the NMR-observable polypeptide segments of rhodanese bound to SR1, we compared the efficiencies of ^{1}H magnetization transfer in backbone ^{15}N–^{1}H moieties by cross-correlated relaxation between ^{1}H–^{15}N dipole–dipole coupling and ^{1}H chemical shift anisotropy interactions [cross-correlated relaxation-induced polarization transfer (CRIPT)] and by ^{1}H–^{15}N scalar couplings [insensitive nuclei enhanced by polarization transfer (INEPT)]. In this approach, the optimal INEPT transfer time, T_I, and the ratio of the optimal CRIPT and INEPT transfer efficiencies, $A_{C/I}$, are measured and compared with theoretical and experimental reference data[25]. For rhodanese bound to SR1, $T_I \approx 3.5$ ms and $A_{C/I} \approx 0.25$ were obtained [Fig. 1(D)], as compared to previously reported values of $T_I \approx 2.5$ ms and $A_{C/I} \approx 0.3$ for hDHFR in complex with SR1.[25] The longer T_I value for rhodanese is due to slower $^{1}H^{N}$ autorelaxation, which indicates that rhodanese retains more flexibility than hDHFR when bound to SR1. The $A_{C/I}$ values for both substrate proteins are small when compared to the

value of $A_{C/I} \approx 0.8$ predicted for ^{15}N–^{1}H moieties immobilized in a 430-kDa complex, indicating that there is significant intracomplex mobility for both substrate proteins.[25]

Effects of covalent cross-linking of rhodanese to SR1

Considering the indication that rhodanese retains significant mobility within the complex with SR1, it seemed of interest to investigate possible correlations with binding and release of the substrate from the apical domains of SR1 within the binary complex. To this end, we collected NMR spectra of rhodanese before and after covalent binding to the apical cavity wall of the protein SR1[T261C], using disulfide crosslinking between cysteines in rhodanese [Fig. 2(A)] and the cysteine at position 261 of the mutant SR1 [Fig. 2(B)]. Following initial data collection with the noncovalent binary rhodanese–SR1 [T261C] complex, the NMR sample was recovered and disulfide-crosslinking was initiated by adding 4 m*M* diamide (see Materials and Methods section).

The 2D [^{15}N,^{1}H]-CRINEPT–HMQC–[^{1}H]-TROSY spectra taken before and after covalent crosslinking were closely similar (Fig. 3), indicating that crosslinking did have at most small effects on the conformational state of the regions of the rhodanese polypeptide chain that are NMR-visible in the noncovalent complex. This provides additional evidence that there is substantial flexibility in parts of the rhodanese bound either covalently or noncovalently to SR1, and indicates that the NMR experiments used here do not yield information on possible release and rebinding of the intact substrate protein within the SR1 cavity. Comparison with Figure 1(A) shows that the Arg side-chain signal [III in Fig. 1(A)] has reduced intensity in the spectrum of the covalent complex, indicating reduced population of the implicated salt bridge (see above) after crosslinking.

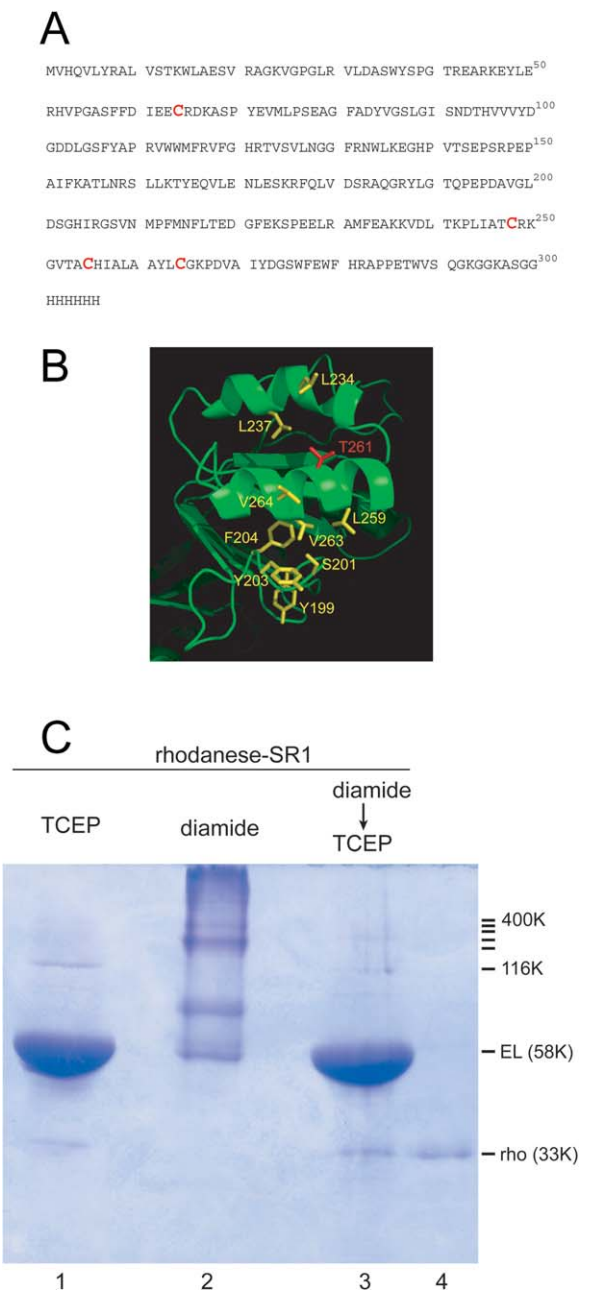

Figure 2. Disulfide crosslinking of a binary complex formed between [u-^{15}N, u-98% ^{2}H]-rhodanese and a SR1 variant containing cysteine in position 261, SR1[T261C]. (A) Primary structure of bovine rhodanese, with the cysteines highlighted in red. (B) Position of the T261C substitution in the apical central cavity, facing the SR1 subunits at the level of helix I (see text). (C) Nonreducing SDS-PAGE of binary complexes before and after disulfide crosslinking: lane 1, noncovalent binary complex after incubation under reducing conditions; lane 2, covalent complex after oxidation with diamide; lane 3, solution of lane 2 after re-reduction of the oxidized complex with an excess of TCEP; lane 4, [u-^{15}N, u-98% ^{2}H]-rhodanese; control lane on the right, migration positions of tandemized GroEL subunits ranging in size from monomer up to heptamer, with molecular sizes of, respectively, 58, 116, 174, 232, 290, 348, and 400 kDa. Note in lane 2 that no free rhodanese was identified after oxidation, confirming oxidative linkage to SR1, and that a species is observed at ~90 kDa, which corresponds to the molecular weight of a 1:1 adduct of rhodanese with a monomeric GroEL subunit. Following addition of an excess of reductant, the original pattern is restored, reflecting reversal of the crosslinks of rhodanese with SR1.

Productivity of the noncovalent binary rhodanese–SR1 complex used for NMR studies

To further qualify the biological significance of the presently reported data, the physiological productivity of the binary SR1 complex with the isotopically labeled rhodanese used for the NMR experiments was monitored by removing aliquots of the SR1–rhodanese complex from the NMR sample tube, diluting the solution to 2 μ*M* concentration of the complex, and adding ATP and GroES. This produced

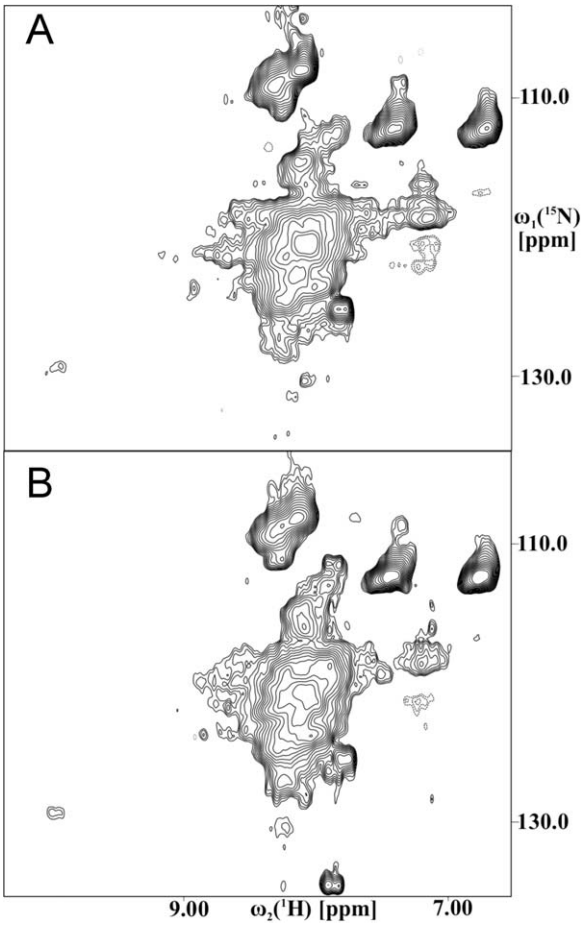

Figure 3. 2D [^{15}N,^{1}H]-CRINEPT–HMQC–[^{1}H]-TROSY spectra of [u-^{15}N, u-98% ^{2}H]-rhodanese in binary complexes with SR1[T261C] at natural isotope distribution before and after disulfide crosslinking. (A) Noncovalent complex. (B) Covalent complex obtained after oxidation with diamide. The same parameter settings were used as in Figure 1(A); see Materials and Methods section.

near-quantitative recovery of native rhodanese, as judged from assaying rhodanese enzymatic activity, whereby this estimate was based on the amount of rhodanese bound to SR1 and the specific activity of native rhodanese. Because native rhodanese is unstable at concentrations above ~20 μ*M* and aggregates even in the presence of a large excess of thiosulfate, it was not possible to follow up on previous experiments with hDHFR[25] and obtain NMR spectra of the renatured substrate.

Conclusions and Outlook

Rhodanese bound noncovalently to SRI shows qualitatively similar behavior to that observed earlier with hDHFR in a corresponding noncovalent binary complex, and a new approach with NMR studies of rhodanese covalently disulfide crosslinked with SR1 enables a more precise interpretation of the data. The observed intracomplex mobility of the rhodanese cannot be rationalized by binding and release of the intact protein from the apical domains of SR1 but must be due to rate processes within the bound substrate. It will be of special interest to further explore how the NMR observations relate to single-molecule studies of long-range fluorescence energy transfer in GroEL-bound rhodanese,[33] which yielded a broad distribution of FRET efficiencies for the bound rhodanese, apparently reflecting an ensemble of differently bound conformations displaying dynamics resembling that of the chaperonin itself (see also Sharma *et al.*[34]).

Materials and Methods

Preparation of the noncovalent rhodanese–SR1 binary complex

Rhodanese bearing a C-terminal 6-His tag was expressed in BL21/DE3 *E. coli* cells. For the production of [u-^{15}N, u-98% ^{2}H]-rhodanese, cells were grown in minimal medium in D_2O, containing $^{15}NH_4Cl$ as the sole nitrogen source and [u-^{2}H] acetic acid as the sole carbon source.[35] Cells were collected and broken in a microfluidizer in 50 m*M* Tris at pH 8.0, containing 1 m*M* dithiothreitol (DTT). The solution was then made 8*M* in urea, 0.1% in Triton X 100, and the suspension was spun at 30,000*g* for 30 min. The supernatant was adjusted to 6*M* in urea and 5 m*M* in imidazole, and applied to Talon resin. The resin was washed with the same solvent and subsequently eluted with 150 m*M* imidazole in 8*M* urea. The thus recovered rhodanese was dialyzed against 4% acetic acid, lyophilized, and stored at −80°C.

[u-100% ^{14}N]-SR1 was prepared by expression from a T7-SR1 plasmid in BL21/DE3 cells grown on minimal glucose medium containing $^{14}NH_4Cl$ as the sole nitrogen source. SR1 was purified from these cells under nondenaturing conditions, as previously described.[24]

For binary complex formation, 4.7 mg of isotope-labeled rhodanese was suspended in 1 mL of 8*M* urea at 22°C to a final protein concentration of 100–150 μ*M*. After 30 min, the suspension was centrifuged at 16,000*g* for 5 min and then diluted 50- to 75-fold into a 2 μ*M* solution of SR1 in buffer A (50 m*M* Tris at pH 7.4, 5 m*M* $Na_2S_2O_4$, 2 m*M* tris(2-carboxylethyl) phosphine (TCEP)). After 30 min, the mixture was centrifuged at 3000*g* for 5 min. The supernatant was first exchanged against buffer A to remove residual denaturant, and the binary complex was then concentrated in the same buffer to 0.15 m*M*. The concentrated complex solution was supplemented with 5% D_2O before the NMR measurements.

Biochemical characterization of covalently crosslinked rhodanese–SR1 complex

To link the rhodanese to the SR1 cavity wall, we used a variant of the SR1 chaperonin that contained,

in addition to the three natural Cys in each subunit, a cysteine introduced by design in position 261 of the apical domain, where it is at the N-terminal end of the helix I and faces the central cavity [see Fig. 2(B)]. In the rhodanese, there are four cysteines available for interaction, where one is in the N-terminal third of the primary structure and three are in the C-terminal third [Fig. 2(A)]. A study examining the ability of bound substrates to undergo disulfide crosslinking to GroEL has shown that only GroEL cysteines positioned in the central cavity wall are accessible to those in a bound substrate protein.[10] Thus, disulfide crosslinking on addition of an oxidant would be expected to occur either among the four cysteines of the bound rhodanese, between one of these cysteines and the SR1-cysteine at position 261, or possibly between several of the rhodanese cysteines and multiple SR1-subunits, as the Cys 261 residues in the seven subunits of SR1 are sufficiently widely apart to be inaccessible to each other.[4]

To assess that oxidation-mediated crosslinking between the substrate protein and the SR1 cavity wall had indeed occurred, aliquots of the rhodanese–SR1[T261C] binary complex were analyzed by nonreducing sodium dodecyl sulfate polyacrylamide gel electrophoresis (SDS-PAGE) in a 2 m*M* solution of the reducing agent TCEP before oxidation, after oxidation with 4 m*M* diamide, and after renewed re-reduction with 10 m*M* TCEP. Prior to oxidation, the binary complex produced bands corresponding to rhodanese [Fig. 2(C), compare lane 1 with rho in the control lane], a heavy band corresponding to monomeric SR1 subunits (compare with EL in the control lane), and a contaminant species of ~120 kDa whose identity is not known. Subsequent to oxidation, both rhodanese and the majority of the SR1 subunits have been displaced into species of larger molecular size, apparently generated by the intended oxidative crosslinking [Fig. 2(C), lane 2]. One product with M ~90 kDa corresponds in size to an SR1 subunit–rhodanese crosslink product, while a multitude of larger species likely comprise rhodanese linked with multiple SR1 subunits. As observed in earlier disulfide crosslinking of binary complexes of rubisco with GroEL[T261C],[3] such oxidized species migrate somewhat heterogeneously, apparently dependent on the nature of the branched structures that are produced. To confirm that the links formed here were indeed reversible disulfide linkages, the oxidization products were re-reduced by incubation with TCEP, which restored the original gel pattern that had been observed prior to oxidation [Fig. 2(C), lane 3].

NMR spectroscopy

All NMR spectra were recorded at 25°C on an AVANCE-800 MHz spectrometer (Bruker Biospin, Billerica, MA) equipped with a triple-resonance probehead and a shielded z-gradient coil. The spectra were processed with the program TOPSPIN (Bruker Biospin, Billerica, MA) and analyzed using the CARA software package.[36]

The following parameters were used for the recording and processing of 2D [^{15}N,^{1}H]-correlation experiments: data size 32 × 1024 complex points, t_{1max} = 9 ms, t_{2max} = 71 ms, 256 transients per t_1 increment. The CRINEPT transfer periods in 2D [^{15}N,^{1}H]-CRINEPT–HMQC–[^{1}H]-TROSY were set to 2.4 ms and the INEPT transfer periods in 2D [^{15}N,^{1}H]-TROSY and 2D [^{15}N,^{1}H]-HSQC to 3.5 ms. Before Fourier transformation, the 2D [^{15}N,^{1}H]-CRINEPT–HMQC–[^{1}H]-TROSY datasets were multiplied along the t_1 dimension with a cosine bell[37] and in the t_2 dimension with an empirically optimized exponential function. The 2D [^{15}N,^{1}H]-TROSY and 2D [^{15}N,^{1}H]-HSQC datasets were processed with the same parameters, except a sine bell shifted by 10[37] was applied along the t_1 dimension.

The coherence transfer data of Figure 1(C) were obtained from two series of measurements with the 2D [^{15}N,^{1}H]-CRIPT–TROSY and the 2D [^{15}N,^{1}H]-INEPT–TROSY experimental schemes, respectively.[26] In these series, the transfer delay, T, was incremented from 0.7 to 6.0 ms in steps of 41 μs. The ^{15}N-evolution delay, t_1, was held constant at 2 μs, so that the pulse sequences effectively yielded one-dimensional spectra. The acquisition time for each of the two series of measurements in Figure 1(D) was about 4 h. The following parameters were used for the data recording and processing: data size along t_2 = 1024 complex points, t_{2max} = 71 ms, 256 transients per experiment. The free induction decays along the t_2 dimension were multiplied with an empirically optimized exponential function.

Acknowledgments

This work was supported by grants from the National Institutes of Health and the Howard Hughes Medical Institute. E.K. was supported by the NIH NRSA fellowship 1F32GM07998. K.W. is the Cecil and Ida M. Green Professor of Structural Biology at The Scripps Research Institute.

References

1. Thirumalai D, Lorimer GH (2001) Chaperonin-mediated protein folding. Annu Rev Biophys Biomol Struct 30:245–269.
2. Hartl FU, Hayer-Hartl M (2002) Molecular chaperones in the cytosol: from nascent chain to folded protein. Science 295:1852–1858.
3. Horwich AL, Farr GW, Fenton WA (2006) GroEL–GroES-mediated protein folding. Chem Rev 106: 1917–1930.
4. Braig K, Otwinowski Z, Hegde R, Boisvert D, Joachimiak A, Horwich AL, Sigler PB (1994) Crystal structure of GroEL at 2.8 Å. Nature 371:578–586.

5. Fenton WA, Kashi Y, Furtak K, Horwich AL (1994) Residues in chaperonin GroEL required for polypeptide binding and release. Nature 371:614–619.
6. Buckle AM, Zahn R, Fersht AR (1997) A structural model for GroEL-polypeptide recognition. Proc Natl Acad Sci USA 94:3571–3575.
7. Wang Z, Feng HP, Landry SJ, Maxwell J, Gierasch LM (1999) Basis of substrate binding by the chaperonin GroEL. Biochemistry 38:12537–12546.
8. Chen L, Sigler PB (1999) The crystal structure of a GroEL/peptide complex: plasticity as a basis for substrate diversity. Cell 99:757–768.
9. Farr G, Furtak K, Rowland MC, Ranson NA, Saibil HR, Kirchhausen T, Horwich AL (2000) Multivalent binding of non-native substrate proteins by the chaperonin GroEL. Cell 100:561–573.
10. Elad N, Farr GW, Clare DK, Orlova EV, Horwich AL, Saibil HR (2007) Topologies of a substrate protein bound to the chaperonin GroEL. Mol Cell 26:415–426.
11. Goloubinoff P, Christeller JT, Gatenby AA, Lorimer GH (1989) Reconstitution of active dimeric ribulose bisphosphate carboxylase from an unfolded state depends on two chaperonin proteins and MgATP. Nature 342:884–889.
12. Zahn R, Plückthun A (1994) Thermodynamic partitioning model for hydrophobic binding of polypeptides by GroEL. II. J Mol Biol 242:165–174.
13. Walter S, Lorimer GH, Schmid FX (1996) A thermodynamic coupling mechanism for GroEL-mediated folding. Proc Natl Acad Sci USA 93:9425–9430.
14. Lin Z, Rye HS (2004) Expansion and compression of a protein folding intermediate by GroEL. Mol Cell 16:23–34.
15. Weissman JS, Rye HS, Fenton WA, Beechem JM, Horwich AL (1996) Characterization of the active intermediate of a GroEL-GroES-mediated protein folding reaction. Cell 84:481–490.
16. Mayhew M, da Silva ACR, Martin J, Erdjument-Bromage H, Tempst P, Hartl FU (1996) Protein folding in the central cavity of the GroEL-GroES chaperonin complex. Nature 379:420–426.
17. Xu Z, Horwich AL, Sigler PB (1997) The crystal structure of the asymmetric GroEL-GroES-$(ADP)_7$ chaperonin complex. Nature 388:741–751.
18. Rye HS, Burston SG, Fenton WA, Beechem JM, Xu Z, Sigler PB, Horwich AL (1997) Distinct actions of *cis* and *trans* ATP within the double ring of the chaperonin GroEL. Nature 388:792–798.
19. Brinker A, Pfeifer G, Kerner MJ, Naylor DJ, Hartl FU, Hayer-Hartl M (2001) Dual function of protein confinement in chaperonin-assisted protein folding. Cell 107: 223–233.
20. Apetri AC, Horwich AL (2008) Chaperonin chamber accelerates protein folding through passive action of preventing aggregation. Proc Natl Acad Sci USA 105: 17351–17355.
21. Martin J, Langer T, Boteva R, Schramel A, Horwich AL, Hartl FU (1991) Chaperonin-mediated protein folding at the surface of groEL through a "molten globule"-like intermediate. Nature 342:36–42.
22. Mendoza JA, Roger E, Lorimer GH, Horowitz PM (1991) Chaperonins facilitate the in vitro folding of monomeric mitochondrial rhodanese. J Biol Chem 266: 13044– 13049.
23. Smith KE, Fisher MT (1994) Interactions between the GroE chaperonins and rhodanese. Multiple intermediates and release and rebinding. J Biol Chem 270: 21517–21523.
24. Weissman JS, Hohl CM, Kovalenko O, Chen S, Braig K, Saibil HR, Fenton WA, Horwich AL (1995) Mechanism of GroEL action: productive release of polypeptide from a sequestered position under GroES. Cell 83: 577–587.
25. Horst R, Bertelsen EB, Fiaux J, Wider G, Horwich AL, Wüthrich K (2005) Direct NMR observation of a substrate protein bound to the chaperonin GroEL. Proc Natl Acad Sci USA 102:12748–12753.
26. Riek R, Wider G, Pervushin K, Wüthrich K (1999) Polarization transfer by cross-correlated relaxation in solution NMR with very large molecules. Proc Natl Acad Sci USA 96:12748–12753.
27. Riek R, Fiaux J, Bertelsen EB, Horwich AL, Wüthrich K (2002) Solution NMR techniques for large molecular and supramolecular structures. J Am Chem Soc 124: 12144–12153.
28. Fiaux J, Bertelsen EB, Horwich AL, Wüthrich K (2002) NMR analysis of a 900K GroEL–GroES complex. Nature 418:207–211.
29. Zahn R, Spitzfaden C, Ottiger M, Wüthrich K, Plückthun A (1994) Destabilization of the complete protein secondary structure on binding to the chaperone GroEL. Nature 368:261–265.
30. Mori S, Abeygunawardana C, Tegoni M, Johnson MO, van Zijl PCM (1995). Improved sensitivity of HSQC spectra of exchanging protons at short interscan delays using a new fast HSQC (FHSQC) detection scheme that avoids water saturation. J Magn Reson B 108: 94–98.
31. Pervushin K, Riek R, Wider G, Wüthrich K (1997) Attenuated T_2 relaxation by mutual cancellation of dipole–dipole coupling and chemical shift anisotropy indicates an avenue to NMR structures of very large biological macromolecules in solution. Proc Natl Acad Sci USA 94:12366–12371.
32. Pervushin K, Wider G, Wüthrich K (1998) Single transition-to-single-transition polarization transfer (ST2-PT) in [^{15}N,^{1}H]-TROSY. J Biomol NMR 12: 345–348.
33. Hillger F, Hänni D, Nettels D, Gesiter S, Grandin M, Textor M, Schuler B (2008) Probing protein–chaperone interactions with single-molecule fluorescence spectroscopy. Angew Chem Int Ed Engl 47:6184–6188.
34. Sharma S, Chakraborty K, Müller BK, Astola N, Tang YC, Lamb DC, Hayer-Hartl M, Hartl FU (2008) Monitoring protein conformation along the pathway of chaperonin-assisted folding. Cell 133:142–153.
35. Fiaux J, Bertelsen EB, Horwich AL, Wüthrich K (2004) Uniform and residue-specific ^{15}N-labeling of proteins on a highly deuterated background. J Biomol NMR 29: 289–297.
36. Keller R (2004) Computer Aided Resonance Assignment. http://cara.nmr.ch/. Accessed June 2011.
37. DeMarco A, Wüthrich K (1976) Digital filtering with a sinusoidal window function: an alternative technique for resolution enhancement in FT NMR. J Magn Reson 24:201–204.